1.E.1:2.I. *Nuclear Physics* **A190** (1972) 229—260; © *North-Holland Publishing Co., Amsterdam*

LEVEL DENSITIES FROM SPECTRA OF DIFFERENT REACTIONS POPULATING THE SAME NUCLEUS

C. C. LU, L. C. VAZ † and J. R. HUIZENGA

Nuclear Structure Research Laboratory, and Department of Chemistry, University of Rochester, Rochester, New York 14627 ††

Received 17 January 1972
(Revised 4 April 1972)

Abstract: Level densities of ^{56}Fe, ^{59}Co, ^{60}Ni, ^{62}Ni, ^{63}Cu and ^{65}Cu are determined from analyses of several charged-particle spectra populating the same residual nucleus. Experimental spectra are reported for the following reactions: ^{56}Fe(α, α′)^{56}Fe, ^{59}Co(p, α)^{56}Fe, ^{59}Co(p, p′)^{59}Co, ^{59}Co(α, α′)^{59}Co, ^{56}Fe(α, p)^{59}Co, ^{62}Ni(p, α)^{59}Co, ^{60}Ni(α, α′)^{60}Ni, ^{63}Cu(p, α)^{60}Ni, ^{62}Ni(p, p′)^{62}Ni, ^{62}Ni(α, α′)^{62}Ni, ^{59}Co(α, p)^{62}Ni, ^{65}Cu(p, α)^{62}Ni, ^{63}Cu(p, p′)^{63}Cu, ^{63}Cu(α, α′)^{63}Cu, ^{60}Ni(α, p)^{63}Cu, ^{65}Cu(p, p′)^{65}Cu, ^{65}Cu(α, α′)^{65}Cu and ^{62}Ni(α, p)^{65}Cu. Each of these experimental spectra is analyzed with an exact theory giving the angular and energy-dependent differential cross sections for compound-nucleus reactions including explicitly the angular momentum. From these analyses we have determined the Fermi-gas level-density parameters: ^{56}Fe, $a = 5.7$ MeV^{-1}, $\Delta = 0.7$ MeV; ^{59}Co, $a = 6.2$ MeV^{-1}, $\Delta = -0.8$ MeV; ^{60}Ni, $a = 6.4$ MeV^{-1}, $\Delta = 1.3$ MeV; ^{62}Ni, $a = 6.4$ MeV^{-1}, $\Delta = 0.5$ MeV; ^{63}Cu, $a = 6.8$ MeV^{-1}, $\Delta = -0.5$ MeV; and ^{65}Cu, $a = 6.6$ MeV^{-1} and $\Delta = -0.5$ MeV. All of the spectra were also analyzed with the conventional slope technique which utilizes the Weisskopf expression for the differential cross sections. The results from such an analysis depend on the form of the pre-exponential term in the level-density formula and may give sizeable errors in the Fermi-gas level-density parameter a. A number of theoretical spectra are computed with the exact theory which explicitly includes angular momentum and these spectra are analyzed with the conventional methods to illustrate the errors introduced when angular momentum is not treated properly for such reactions. An estimate of precompound proton emission is made for several (p, p′) reactions.

E NUCLEAR REACTIONS ^{56}Fe(α, α′)^{56}Fe, ^{59}Co(p, α)^{56}Fe, ^{59}Co(p, p′)^{59}Co, ^{59}Co(α, α′)^{59}Co, ^{56}Fe(α, p)^{59}Co, ^{62}Ni(p, α)^{59}Co, ^{60}Ni(α, α′)^{60}Ni, ^{63}Cu(p, α)^{60}Ni, ^{62}Ni(p, p′)^{62}Ni, ^{62}Ni(α, α′)^{62}Ni, ^{59}Co(α, p)^{62}Ni, ^{65}Cu(p, α)^{62}Ni, ^{63}Cu(p, p′)^{63}Cu, ^{63}Cu(α, α′)^{63}Cu, ^{60}Ni(α, p)^{63}Cu, ^{65}Cu(p, p′)^{65}Cu, ^{65}Cu(α, α′)^{65}Cu and ^{62}Ni(α, p)^{65}Cu, measured, calculated $\sigma(E_{\alpha'})$, $\sigma(E_{\alpha})$, $\sigma(E_{p'})$, $\sigma(E_{p})$. ^{56}Fe, ^{59}Co, ^{60}Ni, ^{62}Ni, ^{63}Cu, ^{65}Cu deduced level density parameters. Isotopically separated targets.

1. Introduction

Level-density parameters, such as the Fermi-gas level-density parameter a or the nuclear temperature T have been determined from particle evaporation spectra for several decades. Most such spectra [1]) have been analyzed with the familiar Weiss-

† NSF Graduate Fellow in Chemistry, 1971–72.

†† Supported in part by the US Atomic Energy Commission.

kopf expression [2]),

$$I(\varepsilon_b)\mathrm{d}\varepsilon_b = \text{const}\ \varepsilon_b \sigma(\varepsilon_b)\omega(U)\mathrm{d}\varepsilon_b, \tag{1}$$

where $I(\varepsilon_b)$is the spectral intensity at channel energy ε_b, $\sigma(\varepsilon_b)$ is the inverse cross section and $\omega(U)$ is the state density in the residual nucleus at excitation energy U. The channel energy ε_b of the emitted particle and the excitation energy U of the residual nucleus are related by

$$U = \varepsilon_p + Q_0 - \varepsilon_b, \tag{2}$$

where ε_p is the particle bombarding energy in the c.m. system. In the derivation of eq. (1) no explicit consideration is given to the role of angular momentum in nuclear reactions. In addition to giving no information on angular distributions, the neglect of angular momentum in eq. (1) may lead to distorted spectra from reactions where appreciable values of angular momentum are involved.

The inclusion of angular momentum effects in compound-nucleus reactions has been explicitly formulated by several authors [3-7]). Such an angular and energy-dependent differential cross section for compound-nucleus reactions including angular momentum is given in appendix A. This formula is similar to the well known Hauser-Feshbach [4]) equation except that the isolated residual levels are replaced by a spin-dependent level density. If eq. (A.1) is integrated over angle, the energy-dependent differential cross section including angular momentum is obtained as given in eq. (A.6). If one assumes that the transmission coefficients depend only on the orbital angular momentum, eq. (A.6) may be reduced to an equation similar to eq. (1) as shown in appendix B under the assumption that the spin-dependent level density has the form

$$\rho(U, I) = (2I+1)\rho(U, I = 0). \tag{3}$$

The resulting equation (B.11) has the density of levels of spin zero replacing the state density of eq. (1).

In the application of eq. (1) to the analyses of experimental spectra different forms of the level density have been used. This has led to some confusion as to the meaning of the derived level-density parameters. A more quantitative analysis of the various expressions will be given later in the paper. However, in order to see the origin of the expressions used in the literature we give the more commonly used level-density equations. The Fermi-gas state density for all states is given by

$$\omega(U) = \tfrac{1}{12}(\pi^2/a)^{\frac{1}{4}}(U+t-\Delta)^{-5/4}\exp\{2[a(U-\Delta)]^{\frac{1}{2}}\}, \tag{4}$$

and the Fermi-gas level density for levels of all angular momenta and both parities is given by

$$\rho(U) = \frac{1}{12\sqrt{2}}\,\frac{\hbar}{\mathscr{I}^{\frac{1}{2}}}(U+t-\Delta)^{-\frac{3}{2}}\exp\{2[a(U-\Delta)]^{\frac{1}{2}}\}, \tag{5}$$

where a, $\mathscr{I}$, t and Δ are the Fermi-gas level density parameter, moment of inertia, thermodynamic temperature and energy-shift parameter, respectively. These quanti-

ties are related to each other by

$$(U-\Delta) = at^2 - t, \tag{6}$$

$$\sigma^2 = \mathscr{I}t/\hbar^2 = 0.0137\, A^{\frac{5}{3}}(\mathrm{MeV}^{-1}) \cdot t\ (\mathrm{MeV}) \tag{7}$$

where a nuclear radius of $1.2\, A^{\frac{1}{3}}$ fm is assumed in the computation of $\mathscr{I}$. In the present paper we treat the parameter Δ as an adjustable parameter to account for both the shell and pairing energy corrections. Hence, the energy shift Δ defines a fictive ground state with respect to the actual ground state. The density of levels of spin I is given by

$$\rho(U, I) = (2I+1)\rho(U, I=0)\exp\left[-I(I+1)/2\sigma^2\right], \tag{8}$$

where σ^2 is the spin cut-off parameter defined by eq. (7). Integration of eq. (8) over all values of I gives the result

$$\rho(U) = 2\sigma^2\rho(U, I=0), \tag{9}$$

and the density of levels of spin I and both parities,

$$\rho(U, I) = \frac{a^{\frac{1}{4}}}{24\sqrt{2}}\,\frac{\hbar^3}{\mathscr{I}^{\frac{3}{2}}}\,(U+t-\Delta)^{-2}(2I+1)\exp\left\{2[a(U-\Delta)]^{\frac{1}{2}} - [I(I+1)/2\sigma^2]\right\}. \tag{10}$$

The constant-temperature level densities are given by

$$\rho(U) = \mathrm{const} \cdot \exp\left[(U-\Delta)/T\right], \tag{11}$$

$$\rho(U, I) = \mathrm{const}'(2I+1)(U+t-\Delta)^{-\frac{1}{4}}\exp\left\{[(U-\Delta)/T] - [I(I+1)/2\sigma^2]\right\}, \tag{12}$$

where T is the nuclear temperature.

Substitution into eq. (1) of one of the Fermi-gas densities allows one to determine the level-density parameter a from a particle evaporation spectrum. A plot of the quantity $\ln\{I(\varepsilon_b) \cdot (U+t-\Delta)^n/\varepsilon_b\sigma(\varepsilon_b)\}$ as a function of $(U-\Delta)^{\frac{1}{2}}$ gives a straight line with a slope equal to $2a^{\frac{1}{2}}$. If one employs the state density of eq. (4), the level density of eq. (5) or the spin-dependent level density of eq. (10), the corresponding values of n will be $\frac{5}{4}$, $\frac{3}{2}$ or 2, respectively. In addition, some authors have set $n = 0$ which assumes that the pre-exponential term in the level-density formula is insignificant in terms of the overall exponential dependence of the level density on U. It is worthwhile to explicitly state that the use of the approximate eq. (B.11) predicts a value of $n = 2$. In a similar way, substitution into eq. (1) of one of the constant-temperature level density formulae given by eqs. (11) and (12) enables one to determine the temperature T from a particle evaporation spectrum. A plot of the quantity $\ln\{I(\varepsilon_b) \cdot (U+t-\Delta)^m/\varepsilon_b\sigma(\varepsilon_b)\}$ as a function of U-Δ (or U) leads to a straight line with slope $1/T$. If eq. (11) is used $m = 0$, and if eq. (12) is used then $m = \frac{1}{2}$. The use of the constant-nuclear-temperature approximation is motivated largely by considerations of simplicity. The argument usually used for substitution of the spin-dependent level density of eq. (10) or (12) into eq. (1) is that for some experimental situations, the evaporated particles go primarily into a narrow region of residual spins.

Due to the complexity of the exact theory and the necessity of computer summations to evaluate the differential cross sections from eq. (A.1), only a few attempts have been made to compare results from the approximate Weisskopf-type equations with the predictions of the exact theory. Although previous calculations by Vonach and Huizenga [8]) indicate differences between the exact and approximate formulas, no systematic attempt was made to interpret the results in terms of the resulting deviations in the level-density parameters. Williams and Thomas [9]) showed that erroneous values of the nuclear level-density parameter a may be obtained when nuclear evaporation spectra are analyzed by the Weisskopf formula without taking proper account of the spin dependence of the level density of the residual nucleus. The latter authors employ an angle-integrated cross-section formula and make theoretical analyses of neutron, proton and α-particle spectra. However, their results are subject to some error since the spin fractionation problem was not treated properly. Gadioli and Zetta [10]), employing an angle-integrated differential cross-section formula also, have reported a theoretical comparison of the level-density parameters a obtained from selected (n, p) and (n, α) reaction spectra when analyzed with approximate formulas of the type given by eq. (1). For a number of reactions the latter authors stated a preference for $n = \frac{3}{2}$. These approximate formulas were later used to analyze experimental data and obtain Fermi-gas level-density parameters [11]).

In this paper we present experimental spectra from (p, p'), (p, α), (α, p) and (α, α') reactions populating levels in the same residual nucleus. The level densities of several nuclei with mass around $A = 60$ are studied by analyses of two, three or four spectra from the above-mentioned reactions. Comparisons of spectra giving the same residual nucleus give a more stringent test of the validity of various approximate formulas. The energy spectra of evaporated particles actually give information on the product of the inverse cross section and the level density. The usual procedure in the evaluation of level densities is to assume that the inverse cross section is the same as the cross section for the nucleus in its ground state. The goodness of this approximation can be studied also by comparing different reactions leading to the same residual nucleus by the emission of different kinds of particles.

Theoretical energy spectra of various evaporated particles have been calculated as a function of angle by performing the summations of eqs. (A.1)–(A.3) by computer. In a similar way, angle-integrated theoretical spectra have been computed with eq. (A.6). These various theoretical spectra were analyzed with the approximate theory of eq. (1) [eq. (B.11)] utilizing different forms of the level density to give effective values of the level-density parameters a and T. Comparisons of such calculations will be discussed for several nuclei. The difference between the input value of the level-density parameter a (or T) in the exact theory and the effective value of a (or T) deduced from the approximate theory depends on several factors. These factors will be discussed in later sections. The experimental spectra were analyzed also with both the exact and approximate theories. Level densities as a function of excitation energy are given for ^{56}Fe, ^{59}Co, ^{60}Ni, ^{62}Ni, ^{63}Cu and ^{65}Cu.

2. Experimental procedure

Proton and α-particle spectra were measured for (p, p′) and (p, α) reactions on targets of ^{59}Co, ^{62}Ni, ^{63}Cu and ^{65}Cu with 13, 13, 12 and 11 MeV protons, respectively. Similar spectra for the (α, p) and (α, α′) reactions on targets of ^{56}Fe, ^{59}Co, ^{60}Ni and ^{62}Ni were studied with 17.2, 14.1, 16.6 and 16.2 MeV α-particle projectiles, respectively. In addition, spectra from the (α, α′) reaction on targets of ^{59}Co, ^{60}Ni, ^{62}Ni, ^{63}Cu and ^{65}Cu were determined with 17 MeV α-particle projectiles. In all of these reactions the projectiles were accelerated to the desired energy with the Emperor tandem Van de Graaff of the University of Rochester.

The self-supporting target foils† required in these experiments have the following thicknesses and isotopic compositions: ^{56}Fe, 0.500 mg/cm^2 and 99.9 at. %; ^{59}Co, 0.542 mg/cm^2 and 100 at. %; ^{60}Ni, 0.485 mg/cm^2 and 99.8 at. %; ^{62}Ni, 0.465 mg/cm^2 and 98.7 at. %; ^{63}Cu, 0.515 mg/cm^2 and 99.7 at. %; ^{65}Cu, 0.517 mg/cm^2 and 99.7 at. %. In all experiments, the target foil was rotated 30° from the position normal to the beam. The particle detectors were placed in back of a 0.32 cm diameter collimator and 15 cm from the target. Beam intensities ranged from 0.05 to 0.35 μA and typical runs lasted about 2 h.

The emitted α-particles were detected by thin surface-barrier detectors with thicknesses just sufficient to stop the most energetic α-particles. The maximum energy deposited in these detectors by protons is of the order of 4.7 MeV. A gate was set to reject these low-energy pulses from protons. Since there are very few α-particles with energy less than 5 MeV due to the Coulomb barrier, the above cut-off has a negligible effect on the α-particle spectra. For the targets, bombarding particles and energies under investigation, the Q-values for emission of deuterons and tritons restrict the energies of these particles to values less than 4.5 MeV. Hence, the α-particle spectra are determined accurately to energies as low as 5 MeV without a particle-identifying telescope.

Two silicon solid-state detectors were used in a $\Delta E - E$ counter telescope to measure the proton spectra. Silicon detectors of 2000 and 3000 μm served as E−counters while the ΔE counters had thicknesses of 42 and 55 μm. A computer program CONTLX was used to generate the identification spectrum and to establish the gate settings for each particle type. The proton data were acquired in an on-line mode with a PDP-8 and PDP-6 computer system. In all cases backgrounds were shown to be small by rotating remotely blank target holders into the target position. Both the proton and α-particle spectra were studied at several angles ranging from 87° to 167°.

The projectile energies were kept low enough so that the effect of second particle emission on most of the spectra was negligible. However, a very small contribution of such particles may be present at the lowest energies of the α-spectra resulting from the 17 MeV α-particle bombardments of the copper isotopes.

† The targets were obtained from the Isotopes Development Centre, Oak Ridge National Laboratory, Oak Ridge, Tennessee.

3. Theoretical calculations

3.1. EXACT THEORETICAL CALCULATIONS OF SPECTRA

Exact theoretical evaporation spectra as a function of angle are calculated for compound-nucleus reactions with eqs. (A.1)–(A.3) which are listed [7]) and described in appendix A. Any form of the spin-dependent level density may be used with these equations and full account is taken of the angular momentum. A computer program MAC 3 was written to perform these calculations. For the calculations of an angle-integrated spectrum given by eq. (A.6), a second computer program, EVAP, was written.

The transition coefficients of the entrance and exit channels, $T_a^{l_a}(\varepsilon_a)$ and $T_b^{l_b}(\varepsilon_b)$, which are required for the above computations, are calculated with an ABACUS II computer program. Optical-model parameters employed in the calculations are those of Perey [12]) for protons, Huizenga and Igo [13]) for α-particles and Bjorklund and Fernbach [14]) for neutrons. The Z-coefficients are generated by a computer program ZCOEFF and stored on two different magnetic tapes corresponding to integer and half-integer spins of the compound nucleus, respectively.

In order to evaluate the energy-dependent differential cross section of eq. (A.6) or the energy and angle-dependent differential cross sections of eqs. (A.1)–(A.3), the parameters of the spin-dependent level density must be specified.

Hence, values must be chosen for the level-density parameter a (or temperature T), shell and pairing energy parameter Δ, and moment of inertia $\mathscr{I}$ for each of the residual nuclei formed by neutron, proton and α-particle emission from the compound nucleus. In practice, the parameters are allowed to vary until the calculated proton and α-particle spectra are in good agreement with both the magnitude and shape of the respective experimental spectra. In a few cases, where the cross section for neutron emission is known experimentally, the additional requirement is made that agreement is obtained between the theoretical and experimental neutron emission cross sections. The inter-relationship between the parameters a and Δ will be discussed in subsect. 4.7.

The sums over the entrance and exit channel spins S_a and S_b are performed from $|I_a - i_a|$ to $|I_a + i_a|$ and $|I_b - i_b|$ to $|I_b + i_b|$, respectively. The MAC3 program includes values of I_b up to 14. In the sums over the entrance orbital angular momentum l_a, the exit orbital angular momentum l_b, and the total angular momentum J, values up to 17 are included in each sum. The restrictions on the upper values of l_a, l_b and J impose no difficulty for the calculations which we report since the transmission coefficients are already zero well below the limiting value. The effect of the upper limit of 14 for I_b was checked and found to be negligible. These results are discussed in subsect. 4.1. The MAC3 program is written to include Legendre polynomials up to B_{12}. However, for most calculations reported here it is sufficient to include terms up to B_6. This is especially true for computation of spectra from reactions which give a small anisotropy or for spectra calculated at a scattering angle near 90°.

3.2. APPROXIMATE THEORETICAL CALCULATIONS OF SPECTRA

As discussed in some detail in appendix B, it is possible to derive an approximate expression relating the energy-dependent differential cross section to the level density by making the assumption that the spin-dependent level density has the form given by eq. (3) [ref. [15])]. The resulting equation (B.11) is similar in form to the well-known Weisskopf expression [2]) given in eq. (1), a formula often used in the analyses of evaporation spectra. However, eq. (B.11) explicitly contains the density of levels of zero spin whereas the Weisskopf formula is derived with the application of detailed balance and contains the total state density. In practice, authors have used a variety of level-density expressions in eq. (1) as discussed in sects. 1 and 4.

4. Results of various types of theoretical calculations

4.1. COMPARISON OF EXACT THEORETICAL RESULTS OBTAINED WITH MAC3 AND EVAP TO EVALUATE THE EFFECT OF THE LIMITING VALUE OF I_2 IN THE MAC3 CALCULATIONS

As described in subsect. 3.1, the computer program MAC3 has been written to calculate exact theoretical evaporation spectra as a function of angle. In order to reduce computer time, a restriction was placed on the maximum allowable value of the spin of levels in the residual nucleus of $I_2 = 14$. In order to investigate whether this limit on I_2 was large enough for the reactions under study, a comparison was made between the results of the angle-integrated cross sections obtained from MAC3 with results obtained from our program EVAP. The latter program was written to give only angle-integrated spectra according to eq. (A.6) and, in addition, all spins I_2 of the residual nucleus allowed by angular-momentum coupling are included. A comparison between the results from the two programs for the ^{56}Fe(α, α')^{56}Fe reaction with 17 MeV α-particle projectiles is shown in table 1. As can be seen, the results are almost identical. Since the (α, α') reaction excites high-spin states with considerable yield, we conclude that the limiting value of $I_2 = 14$ used in the MAC3 calculations is sufficient for the reactions included in the present discussion.

4.2. ROLE OF ISOSPIN IN MAC3 CALCULATIONS

Evidence has been published [16-18]) to show that the $T_>$ composite systems decay preferentially by proton emission. Hence reactions induced with protons lead to an enhancement of the (p, p') cross section due to the isobaric-spin selection rule. The incorporation of isospin into the statistical theory calculation of compound-nucleus decay was accomplished in the following way for the MAC3 program [16]).

In the entrance channel proton projectiles give composite systems with two isospins, $T_<$ and $T_>$, having intensity $2T/(2T+1)$ and $1/(2T+1)$ respectively. The quantities $T_<$ and $T_>$ are equal to $T-\frac{1}{2}$ and $T+\frac{1}{2}$ respectively, where T is the isospin of the target. The decay of the composite system of each isospin is treated separately. The transmission coefficients are assumed to be equal to the conventional optical-model transmis-

TABLE 1

Theoretical energy-dependent differential cross sections calculated with the programs MAC3 and EVAP for the $^{56}Fe(\alpha, \alpha')^{56}Fe$ reaction with 17 MeV α-particle projectiles

U (MeV)	Differential cross section (mb · sr^{-1} · MeV^{-1})	
	EVAP	MAC3
0	0	0
0.5	0.0153	0.0153
1	0.0298	0.0298
1.5	0.0533	0.0533
2	0.0896	0.0896
2.5	0.1283	0.1281
3	0.2192	0.2191
3.5	0.3231	0.3229
4	0.4593	0.4591
4.5	0.6304	0.6300
5	0.8341	0.8336
5.5	1.0605	1.0598
6	1.2876	1.2867
6.5	1.4774	1.4759
7	1.5766	1.5750
7.5	1.5281	1.5265
8	1.3048	1.3032
8.5	0.9492	0.9477
9	0.5745	0.5735
9.5	0.2856	0.2849
10	0.1160	0.1156
10.5	0.0365	0.0364
11	0.0066	0.0066

In the MAC3 program, the upper limit on the spin in the residual nucleus was $I_2 = 14$, while no limit was placed on I_2 in the EVAP program.

sion coefficients weighted by the appropriate Clebsch-Gordan coefficients for isospin coupling. Emission of protons from the $T_<$ composite system of ^{63}Cu to the $T = 3$ levels of ^{62}Ni requires a weighting factor of $\frac{6}{7}$, whereas emission of neutrons to $T = 2$ levels of ^{62}Cu entails a weighting factor of 1. Emission of protons from the $T_>$ composite system of ^{63}Cu to the $T = 3$ levels of ^{62}Ni is characterized by a weighting factor of $\frac{1}{7}$ whereas emission of neutrons to the $T = 2$ and $T = 3$ levels of ^{62}Cu have associated weighting factors of 0 and $\frac{6}{7}$, respectively. The other explicit difference comes in the evaluation of the density of final levels of the various residual nuclei. Account is taken of isobaric spin as well as angular momentum and excitation energy.

The shapes of the theoretical spectra are not changed by the inclusion of isospin into the calculation by the above method. However, the spectral intensities or cross sections may be changed.

4.3. EVAP CALCULATIONS WITH A $(2I+1)$ SPIN-DEPENDENT LEVEL DENSITY AND THE EXTRACTION OF THE LEVEL-DENSITY PARAMETER a WITH EQ. (B.13) AND T WITH EQ. (B.14)

As described in some detail in appendix B, a $(2I+1)$ spin-dependent level density given by eq. (B.1) leads to the energy-dependent differential cross section given in eq. (B.11), an expression similar to the Weisskopf expression. With the above form of the spin-dependent Fermi-gas level density, eq. (B. 13) can be used to extract in an exact manner the corresponding Fermi-gas level-density parameter a. In order to explicitly verify this result, we have generated an angle-integrated theoretical spectrum

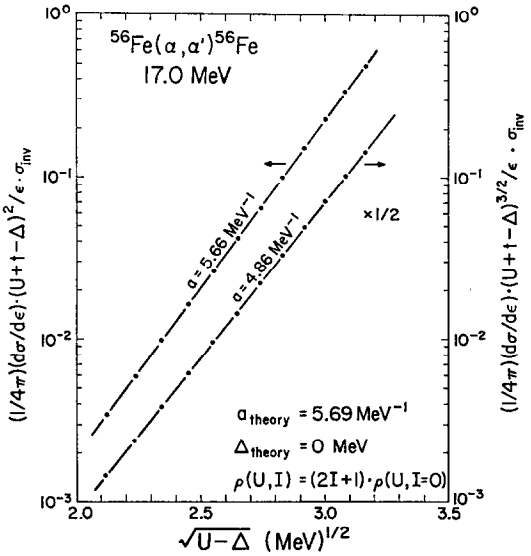

Fig. 1. Conventional analysis of an angle-integrated theoretical spectrum with the familiar Weisskopf intensity expression [see eqs. (1) and (B.13)]. The theoretical spectrum was calculated with the EVAP program [eq. (A.6)] for the ^{56}Fe$(\alpha, \alpha')^{56}$Fe reaction at a bombarding energy of 17 MeV. A $(2I+1)$ spin-dependent level density of the form given by eq. (3) was used in the calculation of the theoretical spectrum. The conventional analysis by the slope technique with $n = 2$ [n is defined as the value of the negative exponent of the pre-exponential energy term of eq. (10)] gives the same value of a as used in the calculation of the theoretical spectrum as one expects for a $(2I+1)$ level density [see eq. (B.12)].

with our program EVAP for a $(2I+1)$ spin-dependent Fermi-gas level density. This was done for the ^{56}Fe$(\alpha, \alpha')^{56}$Fe reaction with α-projectiles of 17 MeV bombarding energy.

The results of the above theoretical spectrum with eq. (B.13) (i.e. with $n = 2$ where n is defined and discussed in sect. 1) are shown in fig. 1. The value of a obtained from the slope of the solid line of fig. 1 is 5.66 MeV^{-1}, a value in excellent agreement with the input value of $a = 5.69$ MeV^{-1} which was used in the EVAP program. Hence, this result is in agreement with expectations and serves as an additional check on the program EVAP. If a value of n different from 2 (see sect. 1) is used, then one

expects the value of a determined from the slope of a plot similar to eq. (B.13) to be different from the input a-value used to generate the theoretical spectrum. A result showing that this is indeed the case is shown in fig. 1 where for $n = \frac{3}{2}$ the slope method gives $a = 4.86\ \text{MeV}^{-1}$ when an input value of $a = 5.69\ \text{MeV}^{-1}$ is used in the theoretical EVAP calculation.

A similar check was made with a constant-temperature level density. A theoretical spectrum for the above reaction is generated with an input of a $(2I+1)$ spin-dependent constant-temperature level density. An analysis of this theoretical spectrum according to eq. (B.14) (i.e. with $m = \frac{1}{2}$ where m is defined and discussed in sect. 1) yields a

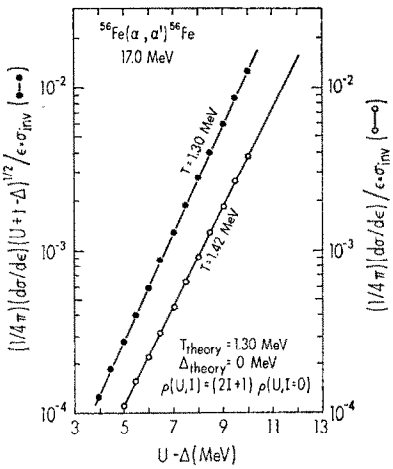

Fig. 2. Similar to fig. 1 except that the constant-temperature form of the nuclear level density is used. The conventional constant-temperature analysis of the theoretical spectrum calculated with $T = 1.30$ MeV gives the same temperature for $m = \frac{1}{2}$ as one expects for a $(2I+1)$ level density.

value of $T = 1.30$ MeV which is in excellent agreement with the input value of $T = 1.30$ MeV. If, on the other hand, the analysis is performed with $m = 0$, a value significantly different from the input value of $T = 1.42$ MeV is obtained. These results are shown in fig. 2.

The results of these calculations confirm that the values of a and T extracted from the slopes of the lines in figs. 1 and 2, respectively, agree with the EVAP input values for a spin-dependent level density with a $(2I+1)$ dependence. However, it is well known that such a spin-dependent level density is unrealistic when large spins are involved. Hence, the values of a and T extracted from plots given by eqs. (B.13) $(n = 2)$ and (B.14) $(m = \frac{1}{2})$, respectively, may be subject to considerable error. This subject will be discussed later.

4.4. CALCULATION OF THE APPARENT VALUES OF a WITH VARIATION IN n

As discussed in sect. 1, a plot of the quantity $\ln\{(\mathrm{d}^2\sigma/\mathrm{d}\varepsilon\mathrm{d}\Omega)\ (U+t-\Delta)^n/\varepsilon_b\sigma(\varepsilon_b)\}$ as a function of $(U-\Delta)^{\frac{1}{2}}$ gives a straight line with a slope equal to $2a^{\frac{1}{2}}$. The value of

n depends on the type of state or level density substituted into eq. (1). It should be emphasized that eq. (1) was developed without consideration of angular momentum. If a $(2I+1)$ spin-dependent level density is assumed, then $n = 2$ as shown in appendix B [see eq. (B.13)]. However, it is well known that such a level density is unrealistic for high-spin levels.

The extraction of the Fermi-gas level-density parameter a from the above type of plot gives an approximate value of a at best. In order to demonstrate the degree of

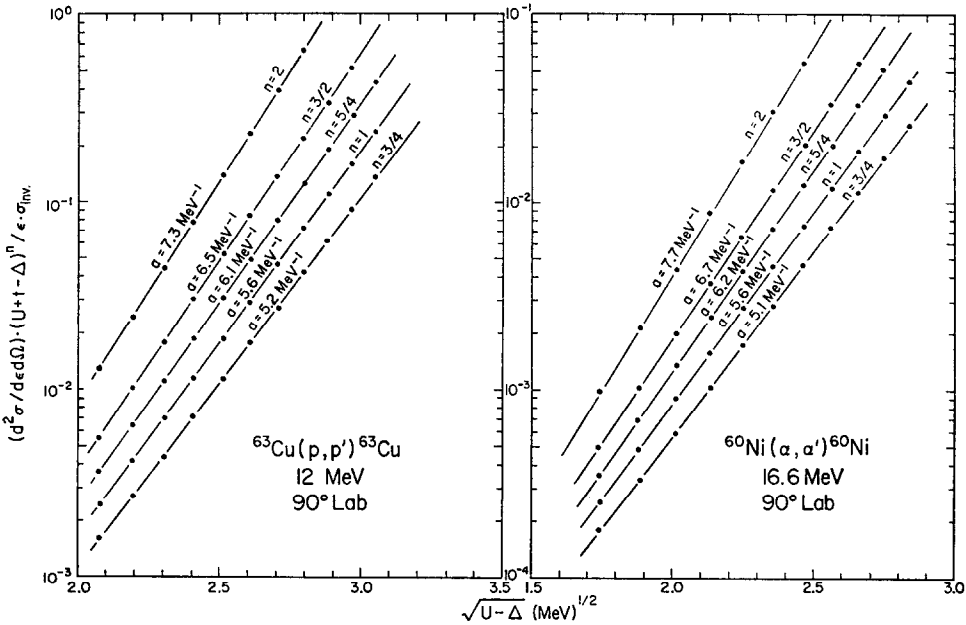

Fig. 3. Dependence of the Fermi-gas level-density parameter a, deduced from the conventional approximate theory on the parameter n. The theoretical spectra analyzed in this figure are calculated with eq. (A.1) and a level density of the form given by eq. (10). The input values of a used in the computation of the theoretical spectra are 6.8 and 5.8 MeV^{-1} for the residual nuclei ^{63}Cu and ^{60}Ni, respectively.

variation of a with n from a Weisskopf formula type analysis, we have calculated theoretical spectra and analyzed these theoretical spectra in the above manner. The results for the ^{63}Cu(p, p')^{63}Cu and ^{60}Ni(α, α')^{60}Ni reactions for values of $n = 2$, $\frac{3}{2}$, $\frac{5}{4}$, 1 and $\frac{3}{4}$ are plotted in fig. 3. The proton projectile energy is 12 MeV and the α-particle projectile energy is 16.6 MeV. The input values of a for ^{63}Cu and ^{60}Ni in the MAC3 program are 6.8 and 5.8 MeV^{-1} respectively. The values of a extracted from the slope technique for ^{63}Cu are 7.3, 6.5, 6.1, 5.6 and 5.2 MeV^{-1} for $n = 2$, $\frac{3}{2}$, $\frac{5}{4}$, 1 and $\frac{3}{4}$ respectively. The values of a extracted from the slope technique for ^{60}Ni are 7.7, 6.7, 6.2, 5.6 and 5.1 MeV^{-1} for $n = 2$, $\frac{3}{2}$, $\frac{5}{4}$, 1 and $\frac{3}{4}$ respectively. These theoretical spectra were analyzed at 90°. Although the results are dependent on angle (see

subsect. 4.6), the 90° results are close to the angle-integrated results. As can be seen from fig. 3, the apparent value of a obtained from the slope method increases with increasing value of n. For the ^{63}Cu(p, p′)^{63}Cu reaction, the correct value of a is obtained for an n-value slightly larger than $\frac{3}{2}$. For the ^{60}Ni(α, α')^{60}Ni reaction, the correct value of a is obtained for an n-value slightly larger than 1.

4.5. COMPARISON OF THEORETICAL SPECTRA CALCULATED WITH THE MAC3 PROGRAM WHERE THE LEVEL DENSITIES OF THE RESIDUAL NUCLEI ARE COMPUTED WITH AND WITHOUT A YRAST LEVEL CORRECTION

In the application of the spin-dependent level density to the statistical theory of nuclear reactions, it has been suggested [19]) that no levels of spin I occur below the yrast energy E_I given by

$$E_I = (\hbar^2/2\mathscr{I})I(I+1), \tag{13}$$

where $\mathscr{I}$ is the moment of inertia. An approximate expression for the spin-dependent level density which takes into account the yrast energy is

$$\rho(U, I) = \frac{a^{\frac{1}{4}}}{24\sqrt{2}} \frac{\hbar^3}{\mathscr{I}^{\frac{3}{2}}} (U+t-\Delta-E_I)^{-2}(2I+1) \exp\{2[a(U-\Delta-E_I])^{\frac{1}{2}}\}. \tag{14}$$

The close relationship between eqs. (14) and (10) is apparent if the quantity $2a^{\frac{1}{4}}(U-\Delta-E_I)^{\frac{1}{2}}$ is expanded with the binomial theorem neglecting the third- and higher-order terms. However, in eq. (14) an yrast energy E_I is subtracted for a level of spin I. The difference between eqs. (10) and (14) is minor except for small excitation energies and large angular momentum values.

The theoretical α-particle energy spectra for the ^{56}Fe(α, α')^{56}Fe reaction with 17 MeV α-particle projectiles were calculated with the spin-dependent level densities given by eqs. (10) and (14). The results for the two level densities are compared in fig. 4 for the angles $\theta_{lab} = 87°$ and 167°. The theoretical spectra are very similar for the two level densities with and without the yrast energy correction.

The effect of the yrast energy correction on the values of a extracted from the slope method is illustrated in fig. 5. The theoretical spectra from the ^{56}Fe(α, α')^{56}Fe reaction with 17 MeV projectiles are analyzed at two lab angles, 87° and 167°, with and without the yrast energy correction. The inclusion of the yrast energy correction reduces the apparent value of a by approximately 5 % at 87° and 2 % at 167°. The corrections for the other reactions we have studied are even smaller and hence we have neglected the yrast energy correction in most of our calculations.

4.6. VARIATION OF THE APPARENT VALUE OF THE FERMI-GAS LEVEL-DENSITY PARAMETER a WITH ANGLE FROM THE SLOPES OF WEISSKOPF FORMULA TYPE PLOTS

The value of a determined from a plot of the quantity $\ln\{(d^2\sigma/d\varepsilon d\Omega)\,(U+t-\Delta)^n/\varepsilon_b\sigma(\varepsilon_b)\}$ as a function of $(U-\Delta)^{\frac{1}{2}}$ depends upon the angle of measurement. The results deduced from the ^{63}Cu(p, p′) reaction at a proton bombarding energy of

12 MeV are shown for 90° and 165° in figs. 3 and 6, respectively, for various values of n. A similar comparison is made for the $^{60}Ni(\alpha, \alpha')^{60}Ni$ reaction at an α-particle bombarding energy of 16.7 MeV in figs. 3 and 6 for angles 90° and 165°, respectively.

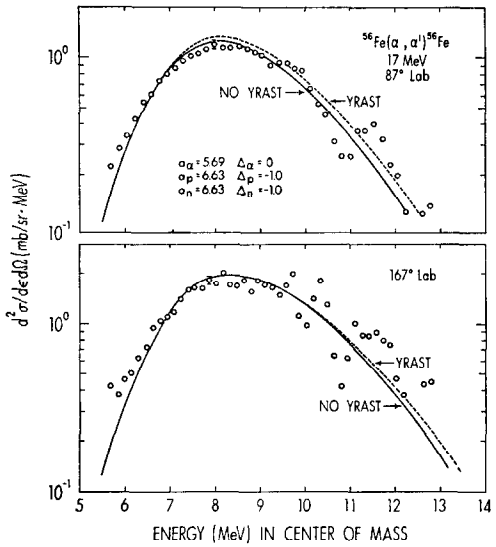

Fig. 4. Comparisons of theoretical spectra calculated with two different forms of the spin-dependent level density, one with and one without a yrast energy correction [see eqs. (14) and (10) respectively].

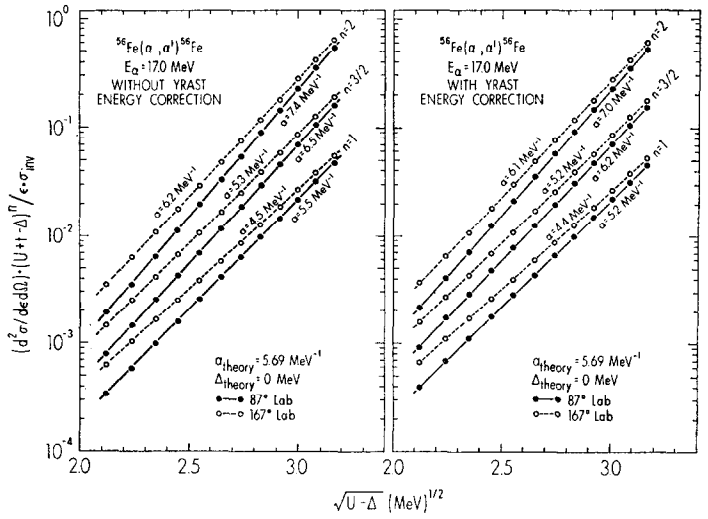

Fig. 5. Effect of the yrast energy correction on the value of the level-density parameter a derived from the approximate conventional analysis. The theoretical spectra are calculated with level densities with and without the yrast energy correction (see fig. 4) and are analyzed by the conventional analysis through the slope technique.

Values of a determined at 87° and 167° for the ^{56}Fe(α, α')^{56}Fe reaction induced with 17 MeV projectiles are displayed in fig. 5. In the ^{56}Fe(α, α')^{56}Fe reaction, for example, a value of n slightly larger than 1 gives the correct value for a at 87° whereas a value of $n \approx \frac{7}{4}$ is needed to give the correct value of a at 167° (see fig. 5).

4.7. INTERDEPENDENCE OF THE APPARENT VALUE OF a AND THE ENERGY SHIFT Δ

It has been reported previously that experimental data which are analyzed to determine level-density parameters can be best fit with a back-shifted Fermi-gas model

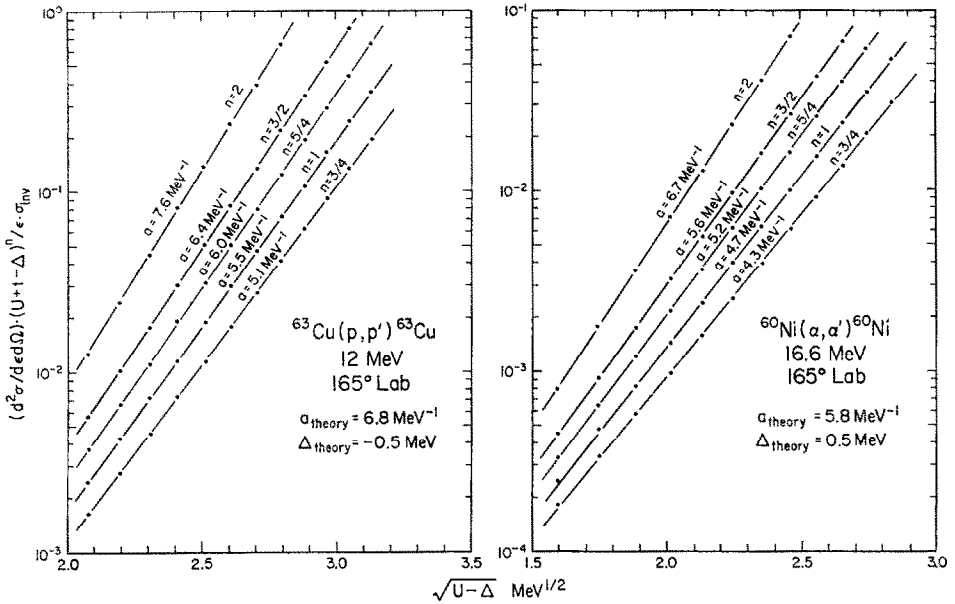

Fig. 6. Dependence of the Fermi-gas level-density parameter a, deduced from the conventional approximate theory, on the parameter n. Same as fig. 3 except that the scattering angle is 165°.

[refs. [20-23,11])]. This empirical energy shift may be understood theoretically as a sum of the shell energy shift and the pairing energy shift. For example, the empirical values of the energy shift (denoted as Δ) for nuclei around $A = 60$ have been estimated previously to be approximately 0.5 MeV for doubly even nuclei and −1.0 MeV for odd-A nuclei.

Due to the uncertainty in the theoretical and experimental values of Δ, we treat it as an adjustable parameter in fitting the experimental spectra with the theory described in appendix A. Unfortunately, the parameters a and Δ are correlated to a certain extent. The dependence of the value of a, determined from a plot of $\ln\{(d^2\sigma/d\epsilon d\Omega)(U+t-\Delta)^n/\varepsilon_b\sigma(\varepsilon_b)\}$ as a function of $(U-\Delta)^{\frac{1}{2}}$, on Δ is illustrated in fig. 7. The theoretical spectra for (p, α), (α, α'), (α, p) and (p, p') reactions populating the residual

nuclei ^{59}Co and ^{62}Ni were calculated at 90° with the MAC3 program by use of eq. (A.1). These theoretical spectra were then analyzed by the slope method with $n = \frac{3}{2}$. Variations in a as a function of Δ by such an analysis for ^{59}Co and ^{62}Ni are shown in fig. 7. The resulting values of $da/d\Delta$ range from -0.5 to -1.0 MeV^{-2}. Hence, for a decrease in Δ of 1 MeV, a increases by about $\frac{3}{4}$ MeV^{-1}.

The relationship between a and Δ deduced from the above slope technique is opposite to the relationship deduced from the exact theory. If a and Δ are adjusted in the fitting of differential cross sections with the exact theory of appendix A, then the

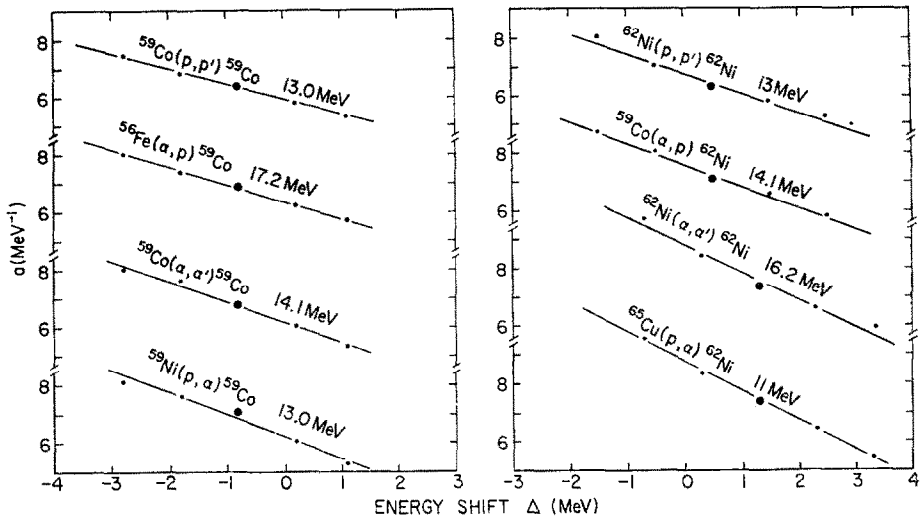

Fig. 7. Dependence of the Fermi-gas level-density parameter a on the value of the energy shift Δ for the conventional analysis of spectra by the slope technique. The theoretical spectra analyzed are generated with eq. (A.1) at a scattering angle of 90° with input values of $a = 6.2$ and 6.4 MeV for ^{59}Co and ^{62}Ni respectively, and energy shifts shown as heavy points (see subsect. 4.7).

quantity $da/d\Delta$ has a positive sign. This is true because the differential cross section is proportional to the total number of levels and increases in both Δ and a have opposite effects on the total number of levels in the residual nucleus. If the level density is determined over a large energy range then information on both a and Δ is obtained [ref. [20])], and at least part of the above ambiguity is removed.

5. Experimental evaporation spectra and their analyses with the exact and approximate theories

5.1. COMPARISON OF EXPERIMENTAL SPECTRA WITH EXACT THEORETICAL CALCULATIONS (MAC3)

All of the experimental spectra have been fitted with the exact theory described in appendix A by utilization of the MAC3 program. The Fermi-gas level-density parameters a and the energy-shift parameters Δ of the residual nuclei were adjusted in the

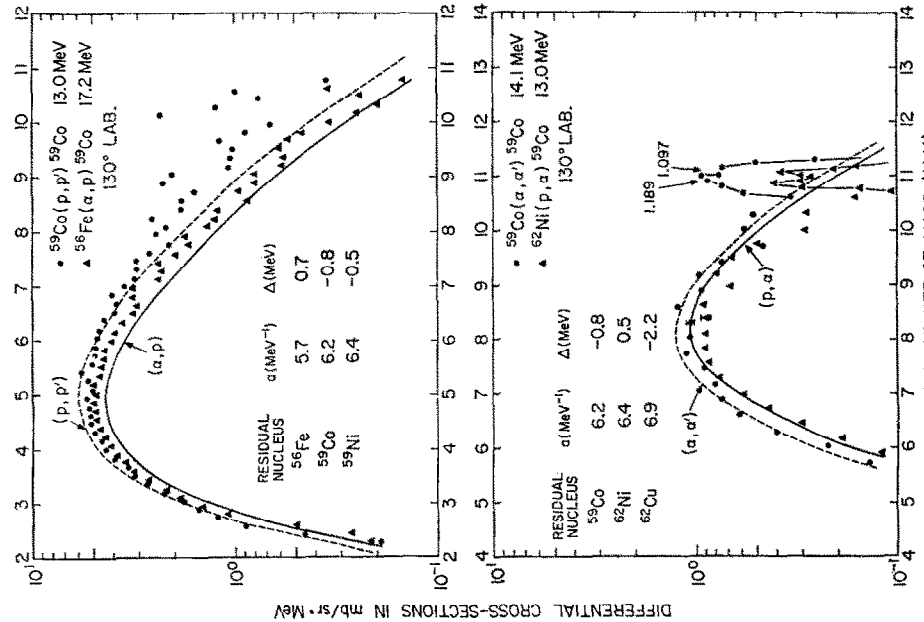

Fig. 8. Comparison of the experimental and theoretical spectra for four different reactions leading to the residual nucleus ^{59}Co. The theoretical spectra based on an exact statistical theory of nuclear reactions including explicitly the angular momentum are calculated with eq (A.1) and the Fermi-gas level-density formula given by eq. (10). The pertinent information is given in the figure.

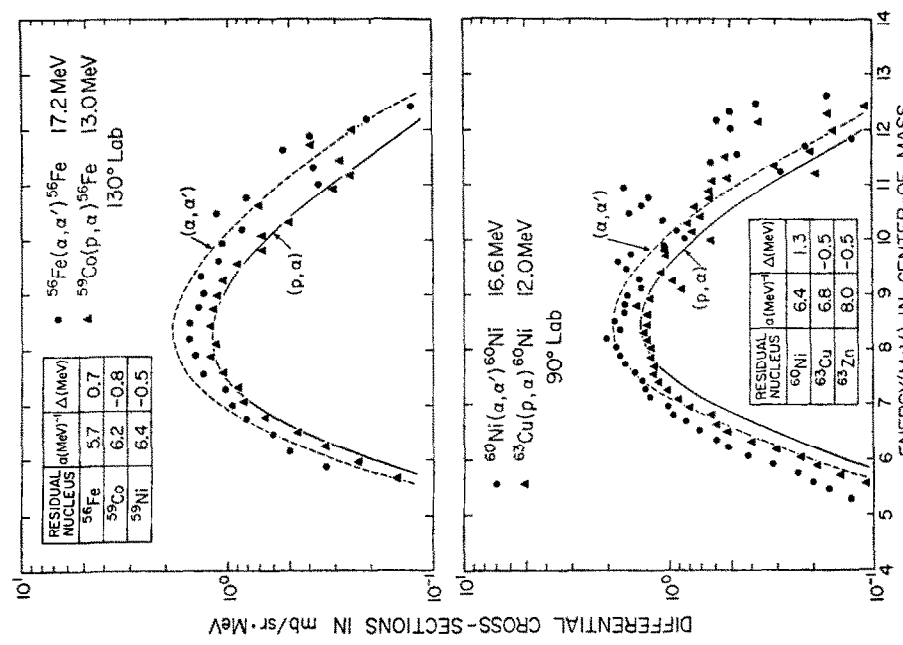

Fig. 9. Comparison of the experimental and theoretical spectra for two different reactions leading to the residual nuclei ^{56}Fe and ^{60}Ni. See caption of fig. 8.

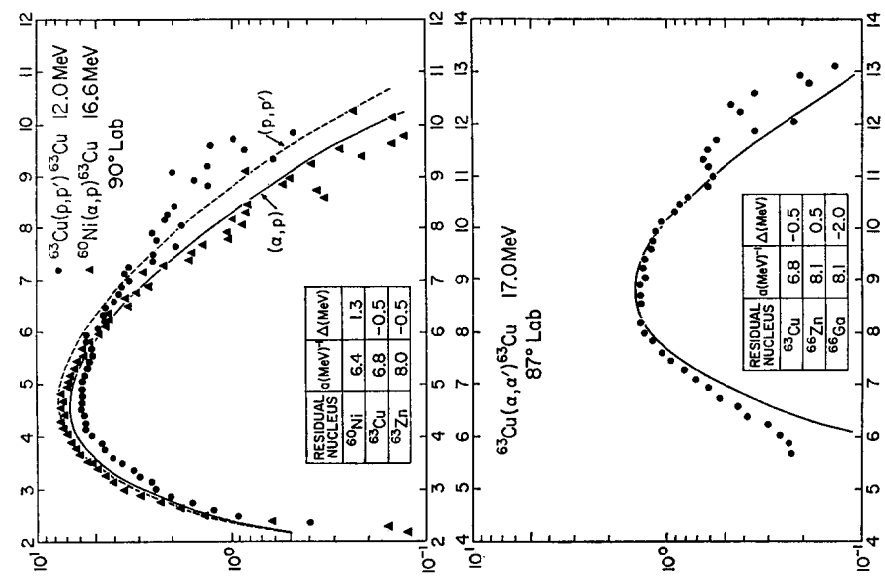

Fig. 11. Comparison of the experimental and theoretical spectra for three different reactions leading to the residual nucleus ^{63}Cu. See caption of fig. 8.

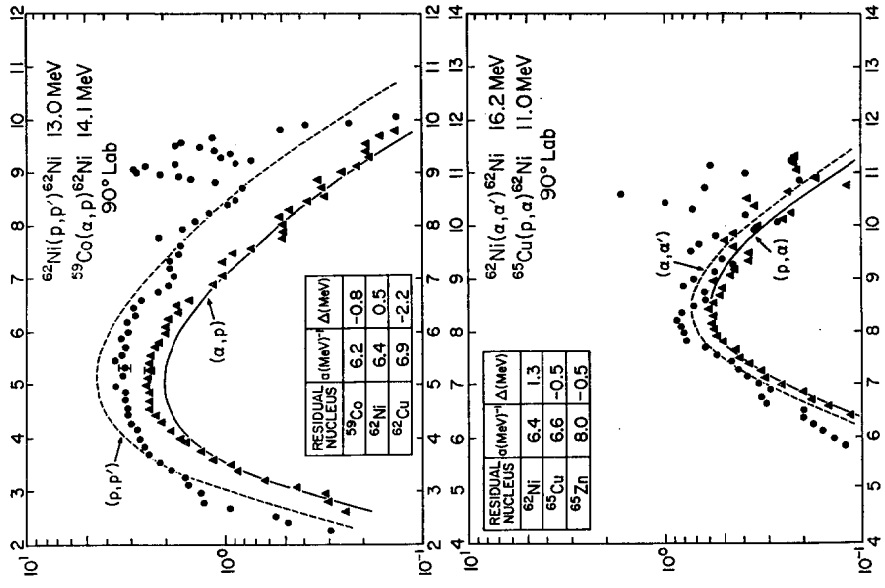

Fig. 10. Comparison of the experimental and theoretical spectra for four different reactions leading to the residual nucleus ^{62}Ni. See caption of fig. 8.

program to give a reasonable agreement between theory and experiment for each spectrum. The results are shown in figs. 8 – 12 for the residual nuclei ^{59}Co, ^{56}Fe and ^{60}Ni, ^{62}Ni, ^{63}Cu and ^{65}Cu respectively. The overall agreement between theory and experiment is very good. However, in a few cases additional small adjustments in the parameters would lead to a better agreement between theory and experiment.

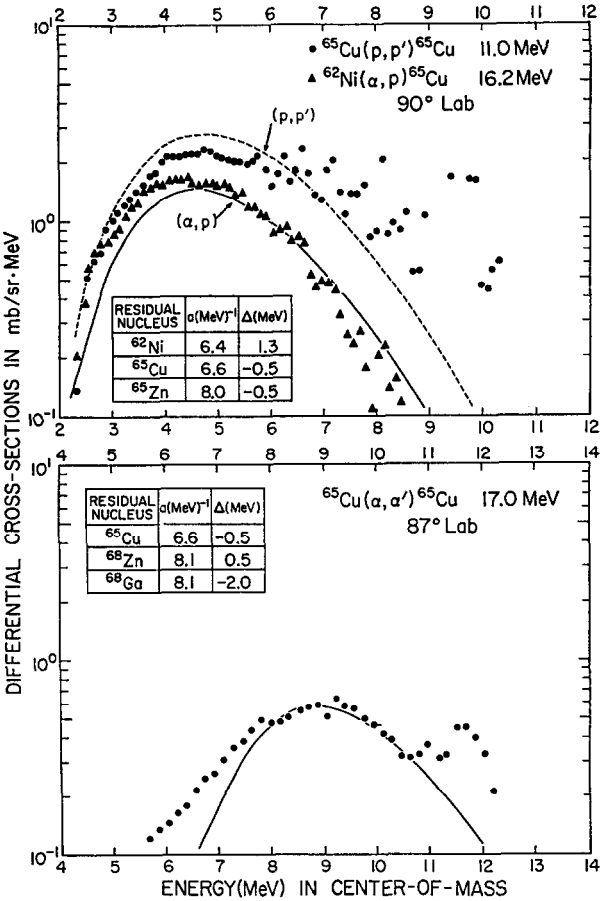

Fig. 12. Comparison of the experimental and theoretical spectra for three different reactions leading to the residual nucleus ^{65}Cu. See caption of fig. 8.

5.2. ANALYSIS OF EXPERIMENTAL CHARGED-PARTICLE SPECTRA BY THE CONVENTIONAL METHOD

In this section we analyze the experimental spectra with an expression of the type given by eq. (1). The determination of the Fermi-gas level-density parameter a is obtained from the slope of the plot of the quantity $\ln\{(\mathrm{d}^2\sigma/\mathrm{d}\varepsilon\mathrm{d}\Omega)\ (U+t-\Delta)^n/\varepsilon_b\sigma(\varepsilon_b)\}$ as a function of $(U-\Delta)^{\frac{1}{2}}$. The results of such analyses for $n = 2$ [see eq. (B.13)] for the residual nuclei ^{59}Co and ^{62}Ni and for $n = \frac{3}{2}$ for the residual nuclei

TABLE 2

Level-density parameters

Reaction	Residual nucleus	Exact analysis of exp. data		Slope method of analysis					
				theor. spectra			exp. spectra		
		a	Δ	$a(n=\frac{3}{2})$	$a(n=2)$	T	$a(n=\frac{3}{2})$	$a(n=2)$	T
^{56}Fe(α, α′)	^{56}Fe	5.7	0.7	6.6		1.18	6.3		1.21
^{59}Co(p, α)	^{56}Fe	5.7	0.7	6.7		1.18	6.7		1.08
^{59}Co(p, p′)	^{59}Co	6.2	−0.8	6.4	7.3	1.40	5.4	5.9	1.50
^{56}Fe(α, p)	^{59}Co	6.2	−0.8	6.9	7.8	1.36	7.5	8.1	1.30
^{59}Co(α, α′)	^{59}Co	6.2	−0.8	6.8	7.6	1.13	7.6	8.2	1.05
^{62}Ni(p, α)	^{59}Co	6.2	−0.8	7.1	7.9	1.10	8.5	9.4	1.04
^{60}Ni(α, α′)	^{60}Ni	6.4	1.3	7.4		1.08	7.4		1.07
^{63}Cu(p, α)	^{60}Ni	6.4	1.3	7.5		1.07	7.2		1.06
^{62}Ni(p, p′)	^{62}Ni	6.4	0.5	6.3	7.4	1.32	6.3	7.4	1.31
^{59}Co(α, p)	^{62}Ni	6.4	0.5	7.1	8.0	1.27	7.2	7.6	1.26
^{62}Ni(α, α′)	^{62}Ni	6.4	1.3	7.4	8.9	1.10	7.1	8.4	1.10
^{65}Cu(p, α)	^{62}Ni	6.4	1.3	7.4	8.4	1.06	7.4	8.3	1.05
^{63}Cu(p, p′)	^{63}Cu	6.8	−0.5	6.7		1.26	5.5		1.39
^{60}Ni(α, p)	^{63}Cu	6.8	−0.5	7.4		1.19	8.4		1.09
^{63}Cu(α, α′)	^{63}Cu	6.8	−0.5	7.5		1.23	7.6		1.14
^{65}Cu(p, p′)	^{65}Cu	6.6	−0.5	6.4		1.28	5.7		1.33
^{62}Ni(α, p)	^{65}Cu	6.6	−0.5	7.0		1.18	8.2		1.08
^{65}Cu(α, α′)	^{65}Cu	6.6	−0.5	7.4		1.20	7.7		1.13

In columns 3 and 4 are listed the level-density parameters a(MeV^{-1}) and Δ(MeV) of each residual nucleus obtained from a comparison of the experimental data with exact theory. These parameters were used to generate theoretical spectra with eq. (A.1). The a (MeV^{-1}) and T (MeV) values derived from these theoretical spectra by the conventional slope technique are listed in columns 5–7. The a (MeV^{-1}) and T (MeV) values derived from the experimental spectra by the conventional slope technique are listed in columns 8–10.

^{56}Fe, ^{59}Co, ^{60}Ni, ^{62}Ni, ^{63}Cu and ^{65}Cu are listed in table 2. Each of the appropriate theoretical spectra obtained from the MAC3 program is analyzed by the above formula and the results are tabulated in table 2. The level-density parameters obtained in subsect. 5.1 were used in the calculations of the theoretical spectra and these parameters are also included in table 2.

As observed earlier for theoretical spectra in figs. 3 and 6, the apparent values of a decrease as n is decreased. This same trend can be seen for the experimental spectra by comparison of the results for $n = \frac{3}{2}$ and $n = 2$ given in table 2. A number of other interesting conclusions may be drawn from the information listed in table 2. First of all, the apparent value of a extracted for a particular nucleus by the slope technique depends on the nuclear reaction producing the residual nucleus. The values of a derived from reactions [(α, α) and (p, α) reactions] in which α-particles populate levels in the residual nucleus give larger values of a than do reactions [(α, p) and (p, p′) reactions] in which protons populate levels in the residual nucleus. It is of

importance to note that this is true for both the experimental and the theoretical spectra.

Both the experimental and the theoretical spectra have been analyzed also with the constant-nuclear-temperature level density. The value of the nuclear temperature T is obtained from the slope of the plot of the quantity $\ln\{(d^2\sigma/d\varepsilon d\Omega)/\varepsilon\sigma_{inv}\}$ as a function of $(U-\Delta)$. Results from plots of this type for the residual nuclei ^{56}Fe, ^{59}Co, ^{60}Ni, ^{62}Ni, ^{63}Cu and ^{65}Cu are given in table 2. Each of the appropriate theoretical spectra obtained from the MAC3 program is analyzed also by the constant-temperature formula above and the results are tabulated in table 2.

5.2.1. *Residual nucleus* ^{59}Co. By fitting the ^{59}Co(p, p')^{59}Co, ^{59}Co(α, α')^{59}Co, ^{56}Fe(α, p)^{59}Co and ^{62}Ni(p, α)^{59}Co reaction spectra with the exact theory, we conclude the level-density parameters $a = 6.2$ MeV^{-1} and $\Delta = -0.8$ MeV give a good description of the level density of the nucleus ^{59}Co. The theoretical spectra (calculated with the level-density parameters listed in fig. 8) and the experimental spectra have been analyzed with the conventional slope technique with $n = 2$ and $n = \frac{3}{2}$. As stated earlier, the apparent values of a decrease as n is decreased. In general, the apparent values of a derived from the theoretical spectra by the slope technique are considerably larger than the input value of a used in the derivation of the theoretical spectra. For the cases where this is true, the value of n must be further reduced to give agreement between the actual value of $a = 6.2$ MeV^{-1} and the value derived from the slope technique. Likewise, to extract realistic values of a from the other experimental data by the slope technique one must use the appropriate value of n for each reaction. The slope obtained from the experimental data for the (p, p') reaction is less than the slope obtained from a similar analysis of the theoretical spectrum. This is contrary to the results for the other three reactions and is probably due to a small percentage of precompound and direct protons in the (p, p') experimental spectrum (see sect. 7).

For the bombarding energies used in the ^{59}Co(α, α')^{59}Co, ^{62}Ni(p, α)^{59}Co, ^{56}Fe(α, p)^{59}Co and ^{59}Co(p, p')^{59}Co reactions, the nuclear temperatures of ^{59}Co deduced from the (α, α') and (p, α) reactions are considerably smaller than those deduced from the (α, p) and (p, p') reactions. It is important to note, however, that reasonably good agreement is obtained between the nuclear temperatures deduced from the experimental and theoretical spectra of a single reaction. Hence, the level-density parameter $a = 6.2$ MeV^{-1} gives a good account of the level density of ^{59}Co for all four reactions. The experimental temperature deduced from the (p, p') reaction is slightly larger than the value from the theoretical spectrum and is due as mentioned earlier to a small amount of precompound and direct protons in the (p, p') spectrum.

5.2.2. *Residual nucleus* ^{62}Ni. Comparisons of the values of a deduced from the experimental and theoretical spectra from the ^{62}Ni(p, p')^{62}Ni, ^{59}Co(α, p)^{62}Ni, ^{62}Ni(α, α')^{62}Ni and ^{65}Cu(p, α)^{62}Ni reactions are given for $n = 2$ and $n = \frac{3}{2}$ in table 2. The values of a and Δ obtained by fitting the experimental spectra with the exact

theory are $a = 6.4$ MeV^{-1} and $\Delta = 0.5$ MeV for the (p, p′) and (α, p) reactions and $a = 6.4$ MeV^{-1} and $\Delta = 1.3$ MeV for the (α, α′) and (p, α) reactions. The theoretical and experimental spectra analyzed with the conventional slope technique for this nucleus give results which are in excellent agreement for all reactions. However, the apparent values of a deduced by this technique are again too large for $n = 2$. This is also true for $n = \frac{3}{2}$ for all the reactions except the (p, p′) reaction where $a = 6.3$ MeV^{-1} is in agreement with the value of $a = 6.4$ stated above and used in the calculation of the theoretical spectra.

The nuclear temperatures of ^{62}Ni determined from the experimental spectra of the ^{62}Ni(p, p′)^{62}Ni, ^{59}Co(α, p)^{62}Ni, ^{62}Ni(α, α′)^{62}Ni and ^{56}Cu(p, α)^{62}Ni reactions are in excellent agreement with the temperatures determined from the respective theoretical spectra derived with a level-density parameter $a = 6.4$ MeV^{-1}. As in the previous case with the nucleus ^{59}Co, the nuclear temperatures of ^{62}Ni deduced from the (α, α′) and (p, α) reactions are smaller than those deduced from the (α, p) and (p, p′) reactions.

5.2.3. *Residual nucleus* ^{56}Fe. The values of the level-density parameters a and nuclear temperatures T derived from conventional analyses of the experimental and theoretical ^{56}Fe(α, α′)^{56}Fe and ^{59}Co(p, α)^{56}Fe spectra are listed in table 2. Again the use of the value $n = \frac{3}{2}$ in the conventional data analysis for reactions in which α-particles populate the residual nucleus gives too large a value of the level-density parameter a. Reasonable agreement is obtained between the results of the analyses of each set of experimental and theoretical spectra. The theoretical spectra are based on a level-density parameter $a = 5.7$ MeV^{-1}.

5.2.4. *Residual nucleus* ^{60}Ni. The values of the level-density parameters a and nuclear temperatures T derived from the conventional analyses of the experimental and theoretical ^{60}Ni(α, α′)^{60}Ni and ^{63}Cu(p, α)^{60}Ni spectra are given in table 2. Excellent agreement between the experimental and theoretical values of a and T are obtained for theoretical spectra calculated with $a = 6.4$ MeV^{-1}. Again for α-particle emission, the value of n in the conventional analysis must be reduced to a value of about $n = 1$ in order to reproduce the value of a used in the calculation of the theoretical spectra.

5.2.5. *Residual nucleus* ^{63}Cu. The value of the level-density parameters a and nuclear temperatures T derived from the conventional analysis of the experimental and theoretical ^{63}Cu(p, p′)^{63}Cu, ^{60}Ni(α, p)^{63}Cu and ^{63}Cu(α, α′)^{63}Cu spectra are listed in table 2. For the ^{63}Cu(p, p′)^{63}Cu reaction the level-density parameter a obtained for the experimental spectrum is smaller than the input value of a because of a contribution of precompound protons. For the ^{60}Ni(α, p)^{63}Cu and ^{63}Cu(α, α′)^{63}Cu reactions, a smaller value of n is required to give agreement between the values of a obtained for the theoretical spectra from the slope technique and the actual input value of a. The values of a obtained from the slope technique for the ex-

perimental and theoretical spectra for each reaction are in reasonable agreement and we conclude that a for ^{63}Cu is 6.8 MeV^{-1}.

5.2.6. *Residual nucleus* ^{65}Cu. The value of the level-density parameter a and nuclear temperature T derived from the conventional analysis of the experimental and theoretical ^{65}Cu(p, p′)^{65}Cu, ^{62}Ni(α, p)^{65}Cu and ^{65}Cu(α, α′)^{65}Cu spectra are given in table 2. Similar trends are observed for ^{65}Cu as those discussed previously for ^{63}Cu. For example, the value of $a = 7.7$ MeV^{-1} deduced from the (α, α′) experimental data by the slope technique with $n = \frac{3}{2}$ is in good agreement with the value of $a = 7.4$ MeV^{-1} deduced by the same technique from the theoretical spectrum calculated with $a = 6.6$ MeV. This again indicates that n must be smaller than $\frac{3}{2}$ for (α, α′) reactions. We conclude that the level-density parameters $a = 6.6$ MeV^{-1} and $\Delta = -0.5$ MeV give a good description of the experimental data.

6. Level densities

Experimental information on the nuclear level densities of the nuclei ^{56}Fe, ^{59}Co, ^{60}Ni, ^{62}Ni, ^{63}Cu and ^{65}Cu obtained from direct level counting [24-26]), high-resolution (p, p)

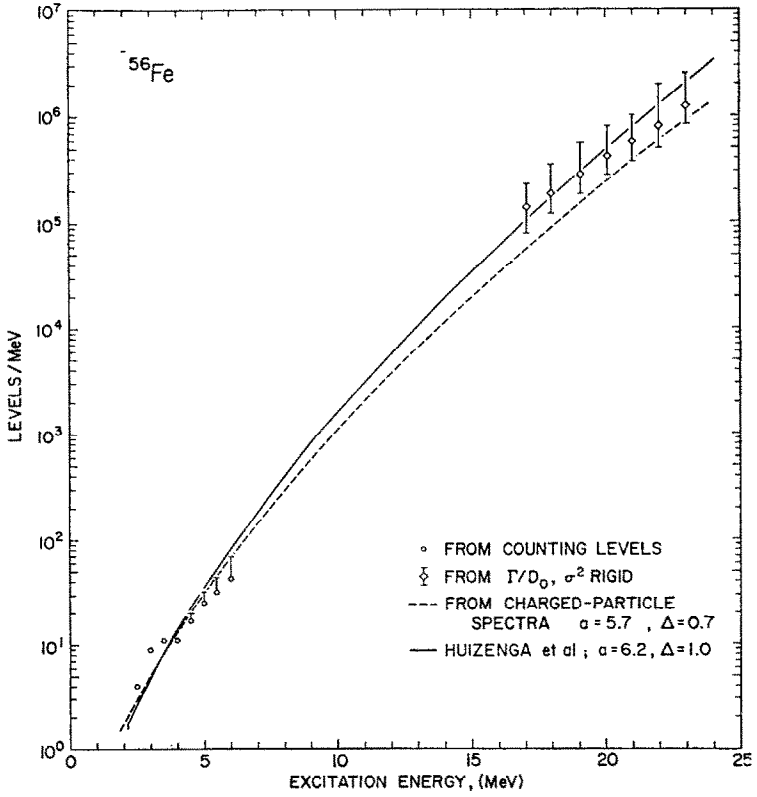

Fig. 13. Plot of the experimental level density of ^{56}Fe as a function of excitation energy. The data of Huizenga *et al.*, are described in ref. [20]).

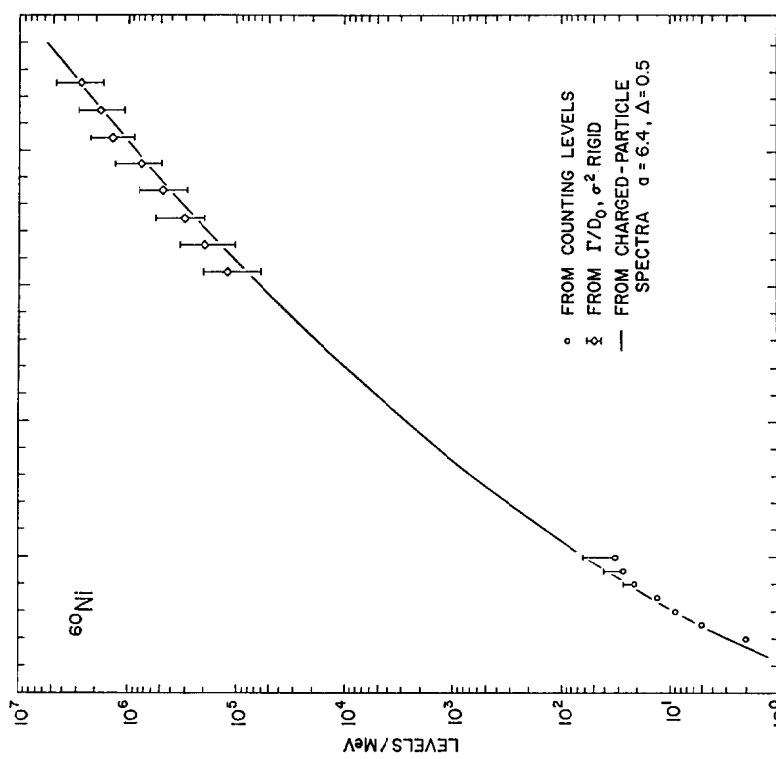

Fig. 15. Plot of the experimental level density of ^{60}Ni as a function of excitation energy.

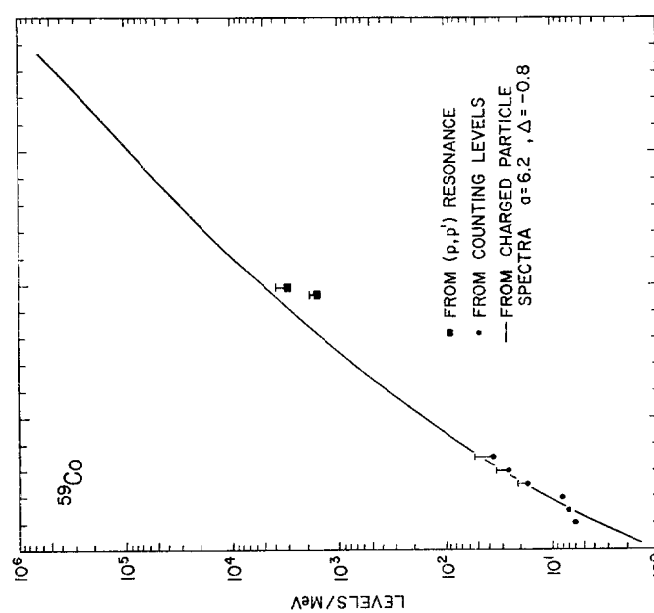

Fig. 14. Plot of the experimental level density of ^{59}Co as a function of excitation energy.

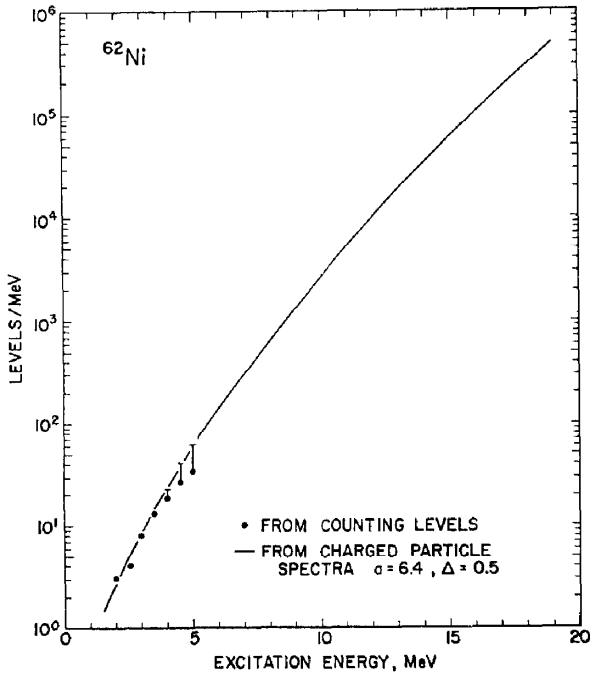

Fig. 16. Plot of the experimental level density of ^{62}Ni as a function of excitation energy.

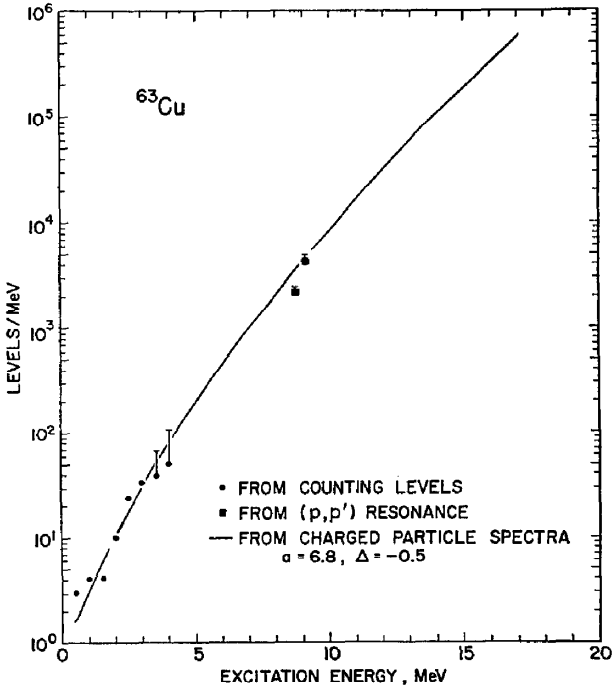

Fig. 17. Plot of the experimental level density of ^{63}Cu as a function of excitation energy.

resonance measurements [27,28]), Ericson fluctuation measurements [20]) and charged-particle spectra are shown in figs. 13–18. The determination of (p, p′) resonances with $l = 0$ on targets of spin zero with high resolution gives the density of levels with spin and parity of $\frac{1}{2}^+$. Such measurements have been made on ^{58}Fe, ^{62}Ni and ^{64}Ni targets giving the density of $\frac{1}{2}^+$ levels at known energies in the nuclei ^{59}Co, ^{63}Cu and ^{65}Cu, respectively. A spin distribution of the form given by eq. (8) and

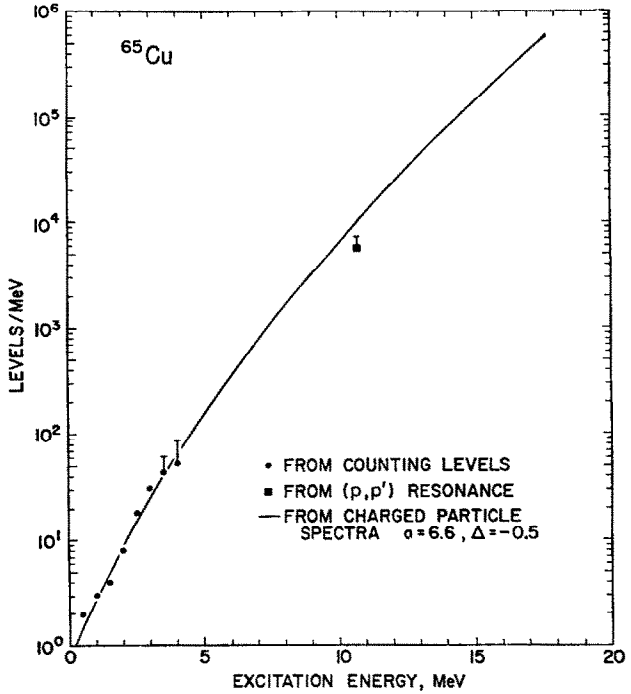

Fig. 18. Plot of the experimental level density of ^{65}Cu as a function of excitation energy.

spin cut-off factor based on a rigid-body moment of inertia are used to calculate the total level densities from the resonance data. Level densities obtained from analyses of the various charged-particle spectra reported in this paper, with the exact theory are shown also in figs. 13–18. The corresponding values of the level-density parameters for the Fermi-gas level-density formula are listed in columns 3 and 4 of table 2.

7. Precompound particle emission

As mentioned earlier there appears to be a small contribution from direct and precompound [29–32]) processes in the (p, p′) spectra, especially at the more forward angles. This is in contrast to the (α, α′), (α, p) and (p, α) reactions (at the bombarding energies of this paper) where the measured angular distributions and energy spectra

are consistent with a compound-nuclear type of process. However, as can be seen from figs. 8 and 10–12 it is not possible to obtain a good fit to the various experimental (p, p′) spectra with the exact statistical theory [eq. (A.1)] when level-density parameters are chosen which fit the (α, α′), (α, p) and (p, α) spectra populating the same residual nucleus.

Estimates of the fractional intensity of the precompound protons have been made by fitting the experimental (p, p′) spectra with a combination of compound-nucleus

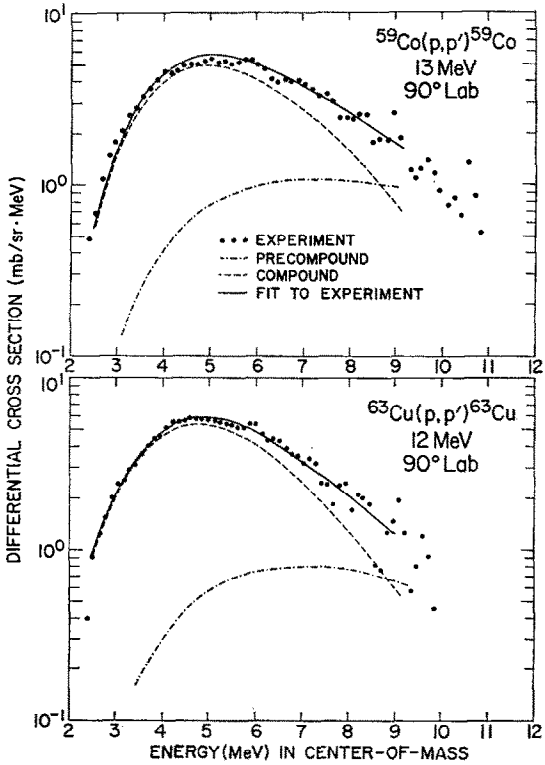

Fig. 19. Fits to the experimental (p, p′) spectra with a combination of compound-nucleus protons and precompound protons. The shapes of the spectra for the compound-nucleus protons were calculated with the level-density parameters derived in this paper. The shapes of the pre-equilibrium spectra were calculated on the basis that the initial configuration is a three-exciton state. The relative intensities of the two different spectra for each reaction were adjusted to give a good fit to the experimental data. For the angle of 90° and the energies listed in the figure, the intensities of precompound protons are 18 % for the ^{59}Co(p, p′)^{59}Co reaction and 14 % for the ^{63}Cu(p, p′)^{63}Cu reaction.

protons and precompound protons. Such a procedure is possible because the theoretical spectra of these two processes are sufficiently different with the precompound spectrum being the harder. The shapes of the spectra for the compound-nucleus protons were calculated with eq. (A.1) and the level-density parameters which are

reported in earlier sections of this paper. The spectral shapes of the precompound protons were computed with the pre-equilibrium theory [29-32]) on the basis that the initial configuration in the composite system is a three-exciton state†. (Calculations were performed also on the assumption that the initial configuration is a two-exciton state. This assumption leads to a harder precompound spectrum and an overall reduction in the relative intensity of precompound protons.) For a particular experimental spectrum the relative intensities of the theoretical compound-nucleus proton spectrum and the pre-equilibrium proton spectrum are adjusted to give a good fit to the experimental data. The resulting fits to experimental spectra are illustrated in fig. 19 for two cases. At a lab angle of 90° we find that for the ^{59}Co(p, p′)^{59}Co (13 MeV), ^{62}Ni(p, p′)^{62}Ni (13 MeV) ^{63}Cu(p, p′)^{63}Cu (12 MeV) and ^{65}Cu(p, p′)^{65}Cu (11 MeV) reactions, the above fitting procedures gives 18 %, 6 %, 14 % and 19 % respectively, for the fractional intensity of pre-equilibrium protons. The fractional contributions of the pre-equilibrium protons are reduced if one integrates over all angles in the backward direction.

8. Conclusions

Analyses of several theoretical charged-particle spectra populating levels in the same residual nucleus have been performed. The residual nuclei studied are ^{56}Fe, ^{59}Co, ^{60}Ni, ^{62}Ni, ^{63}Cu and ^{65}Cu. The conventional analysis of spectra with the Weisskopf expression given by eq. (1) gives a Fermi-gas level-density parameter a or nuclear temperature T which depends on the reaction studied. This is due to the fact that the spin-dependent level density is not adequately accounted for in the derivation of eq. (1). It is shown that the correct value of the Fermi-gas level-density parameter a may be derived from a plot of the quantity $\ln\{(\mathrm{d}^2\sigma/\mathrm{d}\varepsilon\mathrm{d}\Omega)\,(U+t-\Delta)^n/\varepsilon_b\sigma(\varepsilon_b)\}$ as a function of $(U-\Delta)^{\frac{1}{2}}$ by adjustment of the parameter n. However, each different reaction requires a different value of n. For example, (p, p′) reactions require a larger value of n than do (α, α') reactions. Level-density parameters in the literature which are deduced from the conventional analysis of spectra with values of n ranging from 0 to 2 are subject to sizeable errors. In the analyses of our data with the exact theory we treat Δ also as a free parameter to be determined by comparison of the experimental data with the theoretical result. The sign of $\mathrm{d}a/\mathrm{d}\Delta$ is always positive with the exact theory in order to maintain a fixed number of levels (and cross section) at a given energy. The conventional slope technique leads to a negative sign for $\mathrm{d}a/\mathrm{d}\Delta$ which is erroneous. Hence, the slope technique requires that Δ is known.

The conventional analysis of particle evaporation spectra with the simple Weisskopf expression gives erroneous Fermi-gas level-density parameters a. For α-particle reactions of moderate energy the errors in a are up to 50 % depending on the value of n used in the pre-exponential term of the level density. For an accurate determination of the Fermi-gas level-density parameter a from spectra it is necessary

† We wish to thank C. K. Cline for performing the calculations of the pre-equilibrium spectra.

to fit the experimental differential cross section with the exact theory which includes an explicit treatment of the angular momentum and a realistic spin-dependent level density. Descriptions of various computer programs referred to in this paper are available from the authors.

We acknowledge the support of the National Science Foundation to the Nuclear Structure Research Laboratory and the assistance of the operations staff of the Emperor tandem Van de Graaff.

Appendix A

A.1. ANGULAR AND ENERGY-DEPENDENT DIFFERENTIAL CROSS SECTIONS FOR COMPOUND-NUCLEUS REACTIONS

The energy and angular distribution of particles emitted from a compound nucleus in a nuclear reaction is given [7]) by

$$\frac{\mathrm{d}^2\sigma_{\mathrm{ab}}(\varepsilon_{\mathrm{b}})}{\mathrm{d}\varepsilon_{\mathrm{b}}\,\mathrm{d}\Omega_{\mathrm{b}}} = \sum_{\substack{L=0 \\ \text{even}}}^{\infty} B_L(\varepsilon_{\mathrm{b}})P_L(\cos\theta). \tag{A.1}$$

The function $B_L(\varepsilon_{\mathrm{b}})$ is given by

$$B_L(\varepsilon_{\mathrm{b}}) = \tfrac{1}{4}(2I_{\mathrm{a}}+1)^{-1}(2i_{\mathrm{a}}+1)^{-1}k_{\mathrm{a}}^{-2} \times \sum_{S_{\mathrm{a}},S_{\mathrm{b}},I_{\mathrm{b}},l_{\mathrm{a}},l_{\mathrm{b}},J} [G(J)]^{-1}(-)^{S_{\mathrm{a}}-S_{\mathrm{b}}}T_{\mathrm{a}}^{l_{\mathrm{a}}}(\varepsilon_{\mathrm{a}})T_{\mathrm{b}}^{l_{\mathrm{b}}}(\varepsilon_{\mathrm{b}})Z(l_{\mathrm{a}}Jl_{\mathrm{a}}J;\,S_{\mathrm{a}}L) \times Z(l_{\mathrm{b}}Jl_{\mathrm{b}}J;\,S_{\mathrm{b}}L)\rho(U_{\mathrm{b}},I_{\mathrm{b}}), \tag{A.2}$$

and $G(J)$ is given by

$$G(J) = \sum_{\mathrm{b}'}\int_0^{(U_{\mathrm{b}'})_{\max}} \mathrm{d}U_{\mathrm{b}'} \sum_{I_{\mathrm{b}'}=0}^{\infty} T_{\mathrm{b}'}^{l_{\mathrm{b}'}}(\varepsilon_{\mathrm{b}'}) \sum_{S_{\mathrm{b}'}=|J-I_{\mathrm{b}'}|}^{J+I_{\mathrm{b}'}} \sum_{I_{\mathrm{b}'}=|S_{\mathrm{b}'}-i_{\mathrm{b}'}|}^{S_{\mathrm{b}'}+i_{\mathrm{b}'}} \rho_{\mathrm{b}}(U_{\mathrm{b}'},I_{\mathrm{b}'}). \tag{A.3}$$

The quantities $I_{\mathrm{a}}, i_{\mathrm{a}}, J, I_{\mathrm{b}}$ and i_{b} are the spins of the target, projectile, compound nucleus, residual nucleus and the emitted particle respectively; S_{a} and S_{b} are the channel spins in the incident and outgoing channels respectively; l_{a} and l_{b} are the orbital angular momenta of the incident and outgoing particles respectively; k_{a} is the wave number of the incident particles; $P_L(\cos\theta)$ is the Legendre polynomial of order L; $T_{\mathrm{a}}^{l_{\mathrm{a}}}(\varepsilon_{\mathrm{a}})$ and $T_{\mathrm{b}}^{l_{\mathrm{b}}}(\varepsilon_{\mathrm{b}})$ are the transmission coefficients for the projectile and emitted particle respectively, with the channel energies ε_{a} and ε_{b} (the channel energy ε is defined as the sum of the c.m. kinetic energies of the emitted particle and recoil nucleus); $Z(l_{\mathrm{a}}Jl_{\mathrm{a}}J;\,S_{\mathrm{a}}L)$ and $Z(l_{\mathrm{b}}Jl_{\mathrm{b}}J;\,S_{\mathrm{b}}L)$ are the so-called Z-coefficients and are defined as the product of the Racah coefficient W and the Clebsch-Gordan coefficient $(ll00;\,L0)$:

$$Z(lJlJ;\,SL) = (2l+1)(2J+1)(ll00|L0)W(lJlJ;\,SL). \tag{A.4}$$

One of the properties of the Z-coefficients is that they vanish unless $2l+L$ is even. This means that L must be even. This property has the consequence that only the even-

order Legendre polynomials $P_L(\cos\theta)$ are present, i.e. the angular distribution is symmetric around 90° in the c.m. system. The quantity $\rho_b(U_b, I_b)$ is the energy- and spin-dependent level density of the residual nucleus formed by the emission of particles b with channel energy ε_b; the primed notation b′ refers to the different types of emitted particles. The sums in the numerator can be performed independently with respect to the quantum numbers l_a, l_b, J and I_b since the Z-coefficients vanish for combinations of the quantum numbers which violate the conservation of angular momentum.

A.2. ENERGY-DEPENDENT DIFFERENTIAL CROSS SECTION FOR COMPOUND-NUCLEUS REACTIONS

The energy-dependent differential cross section is obtained by integrating eq. (A.1) over all angles. Only the term with $L = 0$ contributes to the energy-dependent differential cross section since the higher-order Legendre polynomials vanish when integrated over the solid angle owing to their orthogonality property. The product of the Z-coefficients reduces to a very simple form since for $L = 0$ the Clebsch-Gordan and the Racah coefficients have the form

$$\begin{aligned}(l l 00|00) &= (-)^l/\sqrt{2l+1},\\ W(lJlJ; S0) &= (-)^{S-l-J}/\sqrt{(2l+1)(2J+1)}.\end{aligned} \tag{A.5}$$

Noting the fact that l_a, l_b and L must obey the triangular relationship and that integration of (A.1) over $d\Omega$ introduces a factor of 4π, the energy distribution of the evaporated particles is given [15]) by

$$\frac{d\sigma_{ab}(\varepsilon_b)}{d\varepsilon_b} = \frac{\pi k_a^{-2}}{(2I_a+1)(2i_a+1)} \sum_{S_a=|I_a-i_a|}^{I_a+i_a} \sum_{l_a=0}^{\infty} T_a^{l_a}(\varepsilon_a) \times \sum_{J=|l_a-S_a|}^{l_a+S_a} \frac{2J+1}{G(J)} \sum_{l_b=0}^{\infty} T_b^{l_b}(\varepsilon_b) \sum_{S_b=|J-l_b|}^{J+l_b} \sum_{I_b=|S_b-i_b|}^{S_b+i_b} \rho_b(U_b, I_b). \tag{A.6}$$

Appendix B

APPROXIMATE FORM OF THE ENERGY-DEPENDENT DIFFERENTIAL CROSS SECTION FOR COMPOUND-NUCLEUS REACTIONS

Eq. (A.6) can be greatly simplified by making the assumption that the spin-dependent level density has a $(2I+1)$ dependence,

$$\rho(U_b, I_b) = (2I_b+1)\rho(U_b, I_b = 0). \tag{B.1}$$

Before proceeding with the derivation we list the following expansions which are needed later:

$$\sum_{I_b=|S_b-i_b|}^{S_b+i_b} (2I_b+1) = (2S_b+1)(2i_b+1),$$

$$\sum_{S_b=|J-l_b|}^{J+l_b}(2S_b+1) = (2J+1)(2l_b+1),$$
$$\sum_{J=|l_a-S_a|}^{l_a+S_a}(2J+1) = (2l_a+1)(2S_a+1),$$
$$\sum_{S_a=|I_a-i_a|}^{I_a+i_a}(2S_a+1) = (2I_a+1)(2i_a+1). \tag{B.2}$$

Making use of the assumption given by eq. (B.1) and the appropriate expressions from eq. (B.2), we simplify first the function $G(J)$ given by eq. (A.3). Implicit of course in the form of eq. (A.3) is the assumption that the transmission coefficients depend only on the orbital angular momenta. The reduced form of $G(J)$ is now

$$G(J) = (2J+1)\sum_{b'}(2i_{b'}+1)\sum_{l_{b'}=0}^{\infty}(2l_{b'}+1)\int_0^{(U_{b'})_{max}} T_{b'}^{l_{b'}}(\varepsilon_{b'})\rho_{b'}(U_{b'}, I_{b'}=0)\mathrm{d}U_{b'}. \tag{B.3}$$

Noting that the total reaction cross section for each type of exit particle b′ is given by an expression

$$\sigma_{b'}(\varepsilon_{b'}) = \pi\lambda\!\!\!^{-2}_{b'}\sum_{l_{b'}=0}^{\infty}(2l_{b'}+1)T_b^{l_{b'}}(\varepsilon_{b'}), \tag{B.4}$$

where $\lambda\!\!\!^{-}_{b}$, is the De Broglie wavelength corresponding to channel energy $\varepsilon_{b'}$, we can write $G(J)$ as

$$G(J) = (2J+1)\left[\sum_{b'}(2i_{b'}+1)\int_0^{(U_{b'})_{max}}\{\sigma_{b'}(\varepsilon_{b'})/\pi\lambda\!\!\!^{-2}_{b'}\}\rho_{b'}(U_{b'}, I_{b'}=0)\mathrm{d}U_b\right]. \tag{B.5}$$

The quantity in the square bracket of eq. (B.5) depends only on the excitation energy of the composite system and is a constant for a particular excitation energy. Hence

$$G(J) = (2J+1)K, \tag{B.6}$$

where K represents a constant equal to the quantity in the square bracket of eq. (B.5).

Substitution of eq. (B.6) into eq. (A.6) and using the spin dependence of eq. (B.1) along with appropriate expressions from eqs. (B.2) and eq. (B.4) for the total reaction cross sections, $\sigma_a(\varepsilon_a)$ and $\sigma_b(\varepsilon)$, we can rewrite eq. (A.6) as

$$\frac{\mathrm{d}\sigma_{ab}(\varepsilon_b)}{\mathrm{d}\varepsilon_b} = \frac{(2i_b+1)\sigma_a(\varepsilon_a)}{K\pi\lambda\!\!\!^{-2}_{b}}\sigma_b(\varepsilon_b)\rho_b(U_b, I_b=0). \tag{B.7}$$

The wavelength $\lambda\!\!\!^{-}_{b}$ is defined by

$$\lambda\!\!\!^{-}_{b} = \hbar/(2\mu_b\varepsilon_b)^{\frac{1}{2}}, \tag{B.8}$$

where μ_b is the reduced mass and ε_b is the outgoing channel energy.

Substitution of eq. (B.8) into eq. (B.7) gives

$$\frac{\mathrm{d}\sigma_{ab}(\varepsilon_b)}{\mathrm{d}\varepsilon_b} = \frac{2\mu_b(2i_b+1)\sigma_a(\varepsilon_a)}{K\pi\hbar^2}\sigma_b(\varepsilon_b)\varepsilon_b\rho_b(U_b, I_b=0). \tag{B.9}$$

Eq. (B.9) may be written in a more simplified form by making the substitution

$$K' = 2\mu_b(2i_b+1)\sigma_a(\varepsilon_a)/K\pi\hbar^2 \tag{B.10}$$

into eq. (B.9). Since for a fixed projectile bombarding energy all the quantities in eq. (B.10) are constants, a new constant K' is defined by this equation. Hence, eq. (B.9) reduces to

$$\frac{d\sigma_{ab}(\varepsilon_b)}{d\varepsilon_b} = K'\sigma_b(\varepsilon_b)\varepsilon_b\rho_b(U_b, I_b = 0). \tag{B.11}$$

Substitution of the spin-dependent level density given by eq. (10) for zero-spin levels into eq. (B.11) gives

$$\frac{d\sigma_{ab}(\varepsilon_b)}{d\varepsilon_b} = K''\sigma_b(\varepsilon_b)\varepsilon_b(U_b+t_b-\Delta_b)^{-2}\exp\{2[a(U_b-\Delta_b)]^{\frac{1}{2}}\}, \tag{B.12}$$

where K'' is a new constant for a particular bombarding energy. From eq. (B.12), the value of the Fermi-gas constant a can be determined from the slope of the straight line obtained from a plot of

$$\ln\{[d\sigma_{ab}(\varepsilon_b)/d\varepsilon_b](U_b+t_b-\Delta_b)^2/\varepsilon_b\sigma_b(\varepsilon_b)\} \text{ versus } (U_b-\Delta_b)^{\frac{1}{2}}. \tag{B.13}$$

If, on the other hand, the constant-temperature level density of eq. (12) is substituted into eq. (B.11), the constant temperature T_b may be obtained from the slope of the straight line by a plot of

$$\ln\{[d\sigma_{ab}(\varepsilon_b)/d\varepsilon_b](U_b+t_b-\Delta_b)^{\frac{1}{2}}/\varepsilon_b\sigma_b(\varepsilon_b)\} \text{ versus } U_b-\Delta_b. \tag{B.14}$$

The latter plot can equally well be made as a function of U_b.

References

1) D. Bodansky, Ann. Rev. Nucl. Sci. **12** (1962) 79;
N. Cindro, Rev. Mod. Phys. **38** (1966) 391
2) V. F. Weisskopf, Phys. Rev. **52** (1937) 295;
J. M. Blatt and V. F. Weisskopf, Theoretical nuclear physics (Wiley, New York, 1952) p. 367
3) L. Wolfenstein, Phys. Rev. **82** (1951) 690
4) W. Hauser and H. Feshbach, Phys. Rev. **87** (1952) 366
5) T. Ericson and V. Strutinsky, Nucl. Phys. **8** (1958) 284; **9** (1959) 689
6) A. M. Lane and R. G. Thomas, Rev. Mod. Phys. **30** (1958) 257
7) A. C. Douglas and N. MacDonald, Nucl. Phys. **13** (1959) 382
8) H. K. Vonach and J. R. Huizenga, Phys. Rev. **149** (1966) 844
9) D. C. Williams and T. D. Thomas, Nucl. Phys. **A107** (1968) 552
10) E. Gadioli and L. Zetta, Nuovo Cim. **51A** (1967) 1074
11) E. Gadioli and L. Zetta, Phys. Rev. **167** (1968) 1016
12) F. G. Perey, Phys. Rev. **131** (1963) 745
13) J. R. Huizenga and G. Igo, Nucl. Phys. **29** (1962) 462
14) F. Bjorklund and S. Fernbach, Phys. Rev. **109** (1958) 1295
15) T. D. Thomas, Ann. Rev. Nucl. Sci. **18** (1968) 343
16) C. C. Lu, J. R. Huizenga, C. J. Stephan and A. J. Gorski, Nucl. Phys. **A164** (1971) 225

17) M. J. Fluss, J. M. Miller, J. M. D'Auria, N. Dudey, B. M. Foreman, Jr., L. Kowalski and R. C. Reedy, Phys. Rev. **187** (1969) 1449
18) L. C. Vaz, C. C. Lu and J. R. Huizenga, Phys. Rev. **C5** (1972) 463
19) J. R. Grover, Phys. Rev. **127** (1962) 2142
20) J. R. Huizenga, H. K. Vonach, A. A. Katsanos, A. J. Gorski and C. J. Stephan, Phys. Rev. **182** (1969) 1149
21) A. A. Katsanos, R. W. Shaw, R. Vandenbosch and D. Chamberlin, Phys. Rev. **C1** (1970) 594
22) H. K. Vonach, A. A. Katsanos and J. R. Huizenga, Nucl. Phys. **A122** (1968) 465
23) H. K. Vonach and M. Hille, Nucl. Phys. **A127** (1969) 289
24) A. A. Katsanos, J. R. Huizenga and H. K. Vonach, Phys. Rev. **141** (1966) 1053
25) R. G. Tee and A. Aspinall, Nucl. Phys. **A98** (1967) 417
26) G. Brown, J. G. B. Haigh, F. R. Hudson and A. E. MacGregor, Nucl. Phys. **A101** (1967) 163
27) D. P. Lindstrom, H. W. Newson, E. G. Bilpuch and G. E. Mitchell, Nucl. Phys. **A168** (1971) 37
28) J. C. Browne, H. W. Newson, E. G. Bilpuch and G. E. Mitchell, Nucl. Phys. **A153** (1970) 481
29) J. J. Griffin, Phys. Rev. Lett. **17** (1966) 478
30) M. Blann, Phys. Rev. Lett. **21** (1968) 1357
31) G. D. Harp, J. M. Miller and B. J. Berne, Phys. Rev. **165** (1968) 1166
32) C. K. Cline and M. Blann, Nucl. Phys. **A172** (1971) 225